Electronic structure and infrared spectrum of a $W_nC^{0,\pm}$ (n = 1–6) cluster*

Zhang Xiu-Rong(张秀荣)[a)†], Kang Zhang-Li(康张李)[a)], and Guo Wen-Lu(郭文录)[b)]

[a)] *School of Mathematics and Physics, Jiangsu University of Science and Technology, Zhenjiang* 212003, *China*

[b)] *School of Materials Science and Engineering, Jiangsu University of Science and Technology, Zhenjiang* 212003, *China*

(Received 20 February 2011; revised manuscript received 17 April 2011)

$W_nC^{0,\pm}$ (n = 1–6) clusters are investigated by using the density functional theory (DFT) at the B3LYP/LANL2DZ level. We find that the neutral, anionic and cationic ground state structures are similar within the same size, and constituted by substituting a C atom for one W atom in the structures of W_{n+1} clusters. The natural bond orbital (NBO) charge analyses indicate that the direction of electron transfer is from the W atom to the 2p orbital of the C atom. In addition, the calculated infrared spectra of the $W_nC^{0,\pm}$ (n = 2–6) clusters manifest that the vibrational frequencies of neutral, anionic and cationic clusters are similar in a range of 80 cm^{-1}–864 cm^{-1}. The high frequency, strong peak modes are found to be an almost stretched deformation of the carbide atom. Finally, the polarizabilities of $W_nC^{0,\pm}$ (n = 1–6) clusters are also discussed.

Keywords: $WnC^{0,\pm}$ (n = 1–6) clusters, electronic structure, infrared spectrum, density functional theory

PACS: 36.40.Cg, 36.40.Vz, 71.15.Mb **DOI:** 10.1088/1674-1056/20/10/103601

1. Introduction

Tungsten carbides have received much attention, owing to their unique physical and chemical properties, such as extreme hardness, high melting point, chemical inertness, interesting catalytic behaviour, etc. Recently, tungsten carbon nanomaterials (nanoparticles, nanotubes and nanocomposites) have aroused considerable interest.[1−8] Scharf *et al.*[9] studied atomic-scale structure of tungsten carbide reinforced nanocomposite diamond-like carbon (DLC) film, showing that there are multiple tungsten and carbon ionized clusters in the tungsten-rich layers. Abad *et al.*[10] studied the optical and the electrical properties of WC/α-C film, which were correlated with the chemical composition and microstructure evolution caused by α-C addition. However, there are no details about tungsten–carbon interactions and mechanisms of tungsten-based carbon nanomaterials. To investigate the above topics, the study of W_nC ionized clusters becomes very important.

While the investigation of bare tungsten and carbon clusters is one of a large number of experimental and theoretical studies,[11−19] there is rather limited data on the structures and properties of W_nC clusters. Experimental spectroscopic data were obtained only for a WC dimer. A resonant two-photon ionization spectroscopy study predicted the ground state, bond length and vibrational frequency of a WC.[20] A synchrotron radiation source was used to measure WC^+ dissociation energies by Fei *et al.*[21] The photoelectron (PE) spectrum of WC^- was reported by Li *et al.*[22] and subsequently measured by Rothgeb *et al.*[23] with a new anion PE spectrum. Samuel *et al.*[24] showed that the spectroscopic transitions arising from WC^- exhibit similarities to those in Pt^- by photoelectron imaging experiment.

With regard to the computational aspect, Balasubramanian[25] computed the spectroscopic constants and potential energy curves of WC using the complete active space multiconfiguration self-consistent field (CASMCSCF) calculation. Stevens *et al.*[26] used the density functional theory (DFT) method with five classes of functional forms to analyse the inter-nuclear distance, the vibrational frequency and the dipole moment of WC. Wang *et al.*[27] also used the DFT method to study neutral, positive and negative WC dimers.

*Project supported by the National Natural Science Foundation of China (Grant No. 51072072).

†Corresponding author. E-mail: zh4403701@126.com

© 2011 Chinese Physical Society and IOP Publishing Ltd

To the best of our knowledge, there have been no studies on the W_nC cluster. The aim of the present paper is to perform systematic calculations on the neutral and charged $W_nC^{0,\pm}$ (n = 1–6) cluster. We present the ground state structure, the electronic structure, the infrared (IR) vibration spectrum and the static polarizability of the $W_nC^{0,\pm}$ (n = 1–6) cluster, which provide an effectibe way to understand the rich tungsten cases of tungsten carbide and to find new functional materials.

2. Computational details

Our previous computations[12,13,28] on the W_n clusters have shown that the B3LYP and BPW91 functions can provide reliable qualitative results. For the $W_nC^{0,\pm}$ (n = 1–6) cluster system, we used the DFT with the un-restricted B3LYP exchange-correlation potential in the Gaussian 03 package[29] and used the effective core potential (ECP) LANL2DZ basis sets,[30] which provide an effective way to reduce difficulties in calculations of the two-electron integrals caused by heavy transition metal atoms. To show the suitability of the methods used in our systems, the experimental data and some theoretical values of bond length, vibrational frequencies and dissociation energies for the $WC^{0,\pm}$ dimer are listed in Table 1. A comparison between the results obtained with different functionals with the same basis set (B3LYP/LANL2DZ and BPW91/LANL2DZ) and the same functional with different basis sets (B3LYP/LANL2DZ and B3LYP /Gen) shows that the calculated values at the B3LYP/LANL2DZ level are in good agreement with the available experimental results, indicating that our calculations are reliable and accurate, which will provide reliable data for the $W_nC^{0,\pm}$ (n = 1–6) cluster.

Table 1. Comparison of bond length (r_e), vibration frequency (ω_e), and binding energy (D_0) of $WC^{0,\pm}$ dimer between experimental data and theoretical values (1 Å=0.1 nm).

	WC			WC^-			WC^+		
	r_e/Å	ω_e/cm^{-1}	D_0/eV	r_e/Å	ω_e/cm^{-1}	D_0/eV	r_e/Å	ω_e/cm^{-1}	D_0/eV
Exp.	1.7135[a]	983.2		1.771[b]					3.86±0.35[c]
B3LYP/LANL2DZ	1.736	988.1	4.69	1.757	1064.6	5.89	1.821	915.2	3.78
BPW91/LANL2DZ	1.737	1007.7	4.28	1.751	1075.3	5.13	1.693	1186.9	4.05
B3LYP/Gen[d]	1.704	1009	5.22	1.759	940	5.50	1.686	1060	6.69

[a] Ref. [20], [b] Ref. [23], [c] Ref. [21], [d] Gen (LANL2DZ for the W atom and 6-311+G(df) for the C atom) Ref. [23].

3. Results and discussion

3.1. Geometrical structure

We optimize the geometries of $W_nC^{0,\pm}$ (n = 2–6) clusters from as many as possible starting geometries including both two- and three-dimensional structures in order to avoid trapping into local minima. The geometrical structures of the ground state for $W_nC^{0,\pm}$ (n = 2–6) cluster are shown in Fig. 1. The neutral, anionic and cationic ground state structures are similar within the same size, except for $W_4C^{0,\pm}$ cluster. When $n > 3$, the clusters each undergo a transition from a two-dimensional structure to a three-dimensional structure.

Compared with pure tungsten clusters, the $W_nC^{0,\pm}$ (n = 2–6) clusters have similar geometries to those of W_{n+1} clusters (Fig. 1). They are constituted by substituting the C atom for one W atom in the structures of W_{n+1} clusters, accompanied by more or less distortion in the clusters, which is the same as other TM_nC (Fe, Co and Ni, n = 2–6) clusters.[31] Figure 1 also shows that most of the $W_nC^{0,\pm}$ (n = 1–6) clusters have relatively low spin: singlet or triplet for the neutral clusters, and doublet or quartet for the ionic clusters. This is different from the high spin coupling of $Fe_nC^{0,\pm}$ cluster[32] due to the fact that $W_nC^{0,\pm}$ tends to have a sufficient bonding orbital for all the valence electrons and form d–d and p–d bonds, leaving fewer un-paired electrons.

3.2. Electronic structure

Table 2 shows the natural bond orbital (NBO) charge populations of $W_nC^{0,\pm}$ (n = 1–6) clusters. The formal electron configurations for the W and C atoms will be $5d^46s^2$ and $2s^22p^2$, respectively. As shown in Table 2, compared with the orbital populations of these formal electron configurations, the populations of 6s (W atom) and 2s (C atom) orbitals decrease,

whereas the orbital populations of almost all of the 5d (W atom) and 2p (C atom) increase. For neutral W_nC ($n = 1$–6) clusters, the population of 6s orbital on W atom is less than 1.2 and that of 5d orbital is more than 4.4. The population of the 2s orbital on the C atom decreases gradually from 1.87 to 1.54 while that of the 2p orbital increases gradually from 2.56 to 3.14 with cluster size increasing. It is easy to find that the obtained population of the 2p orbital is more than the loose population of the 2s orbital in C atom, so we can say that the direction of charge transfer is from W atom to 2p orbital of C atom.

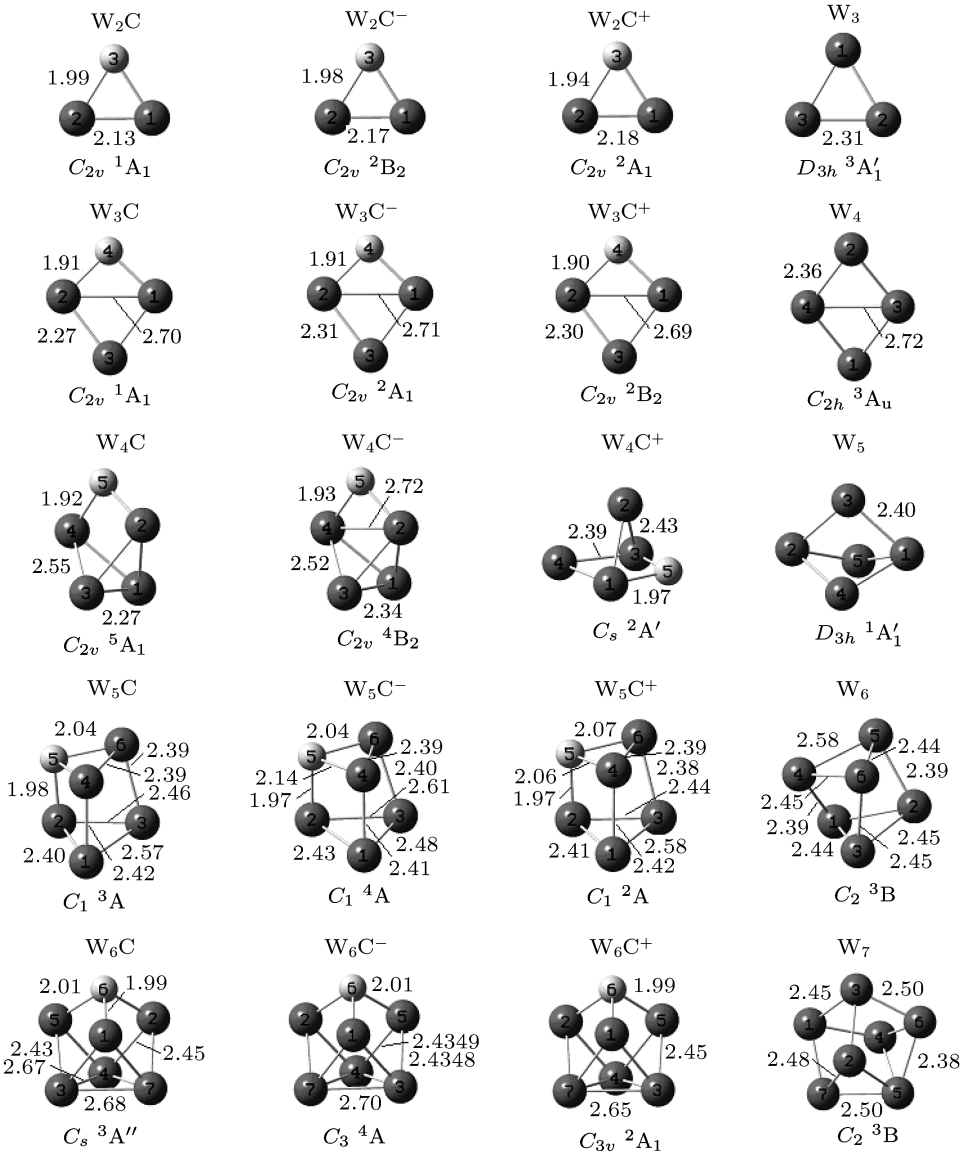


Fig. 1. Ground state structures of $W_nC^{0,\pm}$ ($n = 2$–6) and $W_n{}^{0,\pm}$ ($n = 3$–6) clusters (bond length: Å).

The natural charge of each atom of the $W_nC^{0,\pm}$ ($n = 1$–6) clusters is listed in Table 2. Note that the charge on the W atom in $W_nC^{0,\pm}$ ($n = 1$–6) clusters ranges from −0.29 to 0.97, and the positive charge is higher than that on the W atom in W_nNi_m clusters.[33] In WC^+ dimer, the C atom charge ranges from −0.84 to 0.03, and only positive charge exists on the C atom. For $n \leq 4$ clusters series, the W atom charges of neutral and cationic clusters are positive. As for $n > 4$ cluster series, the charge of W atom which is the neighbourhood with C atom is positive. This proves charge transfer from W to C again.

According to the NBO analyses, there are two interaction patterns that can be used to interpret charge transfer. One is the strong donor–acceptor interaction, such as between lone-pair electrons on W and C atom, σ_{W-C} and π^*_{W-W} orbitals, and the other is the formation of the covalent bond depending on the number and the position of the atoms. The second-order interaction energy (E^2) and Wiberg bond index (WBI) are used

to reveal the strength of donor–acceptor interaction and the covalent bond. The bigger value shows a stronger interaction.

Table 2. Natural electron configurations and charges of $W_nC^{0,\pm}$ (n = 1–6) clusters.

Cluster	Atom	Electron configuration	Charge	Cluster	Atom	Electron configuration	Charge
WC	W	$6s^{0.91}5d^{4.64}6p^{0.04}7s^{0.01}$	0.45		W_3	$6s^{1.10}5d^{4.87}6p^{0.05}6d^{0.02}$	–0.01
	C	$2s^{1.87}2p^{2.56}3s^{0.03}$	–0.45		W_4	$6s^{1.01}5d^{4.73}6p^{0.03}7s^{0.01}6d^{0.02}$	0.24
WC^-	W	$6s^{1.76}5d^{4.44}6p^{0.11}7s^{0.01}$	–0.29		C_5	$2s^{1.61}2p^{3.13}3p^{0.02}$	–0.75
	C	$2s^{1.86}2p^{2.82}3s^{0.03}$	–0.71		W_6	$6s^{0.90}5d^{4.87}6p^{0.03}6d^{0.02}$	0.23
WC^+	W	$6s^{0.78}5d^{4.26}6p^{0.01}$	0.97	W_5C^-	W_1	$6s^{1.21}5d^{4.90}6p^{0.06}6d^{0.02}$	–0.15
	C	$2s^{1.68}2p^{2.29}$	0.03		W_2	$6s^{1.08}5d^{4.83}6p^{0.04}7s^{0.01}6d^{0.03}$	0.04
W_2C	W_1W_2	$6s^{0.97}5d^{4.66}6p^{0.04}$	0.36		W_3	$6s^{1.20}5d^{4.96}6p^{0.05}7s^{0.01}6d^{0.02}$	–0.22
	C_3	$2s^{1.87}2p^{2.82}3s^{0.02}3p^{0.01}$	–0.72		W_4	$6s^{1.10}5d^{4.78}6p^{0.04}7s^{0.01}6d^{0.02}7p^{0.01}$	0.07
W_2C^-	W_1W_2	$6s^{1.33}5d^{4.68}6p^{0.09}7s^{0.01}6d^{0.01}$	–0.08		C_5	$2s^{1.60}2p^{3.18}3p^{0.02}$	–0.80
	C_3	$2s^{1.84}2p^{2.97}3s^{0.02}$	–0.84		W_6	$6s^{1.03}5d^{4.88}6p^{0.03}6d^{0.02}$	0.07
W_2C^+	W_1W_2	$6s^{0.81}5d^{4.50}7p^{0.03}$	0.70	W_5C^+	W_1	$6s^{1.12}5d^{4.83}6p^{0.03}6d^{0.01}$	0.02
	C_3	$2s^{1.68}2p^{2.70}3s^{0.01}3p^{0.01}$	–0.40		W_2	$6s^{0.67}5d^{4.73}6p^{0.03}6d^{0.02}$	0.57
W_3C	W_1W_2	$6s^{1.18}5d^{4.59}6p^{0.01}7s^{0.01}6d^{0.01}$	0.24		W_3	$6s^{0.85}5d^{4.88}6p^{0.05}6d^{0.01}$	0.24
	W_3	$6s^{1.07}5d^{4.85}6p^{0.03}6d^{0.01}$	0.07		W_4	$6s^{0.68}5d^{4.79}6p^{0.03}6d^{0.01}$	0.52
	C_4	$2s^{1.69}2p^{2.84}3s^{0.01}3p^{0.01}$	–0.55		C_5	$2s^{1.61}2p^{3.07}3p^{0.02}$	–0.70
W_3C^-	W_1W_2	$6s^{1.40}5d^{4.61}6p^{0.03}7s^{0.01}6d^{0.02}$	–0.04		W_6	$6s^{0.84}5d^{4.81}6p^{0.02}6d^{0.02}$	0.34
	W_3	$6s^{1.36}5d^{4.89}6p^{0.03}7s^{0.01}6d^{0.03}$	–0.28	W_6C	W_1	$6s^{0.73}5d^{4.87}6p^{0.04}6d^{0.02}$	0.38
	C_4	$2s^{1.68}2p^{2.93}3s^{0.01}3p^{0.01}$	–0.64		W_2W_5	$6s^{0.87}5d^{4.84}6p^{0.03}6d^{0.02}$	0.27
W_3C^+	W_1W_2	$6s^{0.70}5d^{4.66}6p^{0.02}6d^{0.01}$	0.66		W_3W_7	$6s^{0.99}5d^{5.05}6p^{0.05}6d^{0.02}$	–0.07
	W_3	$6s^{1.08}5d^{4.75}6p^{0.02}6d^{0.01}$	0.18		W_4	$6s^{0.97}5d^{5.06}6p^{0.05}6d^{0.02}$	–0.07
	C_4	$2s^{1.71}2p^{2.76}3s^{0.01}3p^{0.01}$	–0.50		C_6	$2s^{1.54}2p^{3.14}3p^{0.03}$	–0.71
W_4C	W_1W_3	$6s^{1.10}5d^{4.80}6p^{0.05}6d^{0.02}$	0.05	W_6C^-	W_1	$6s^{0.98}5d^{4.85}6p^{0.04}7s^{0.01}6d^{0.03}\ 7p^{0.01}$	0.13
	W_2W_4	$6s^{0.85}5d^{4.83}6p^{0.05}7s^{0.01}6d^{0.02}$	0.28		W_2	$6s^{0.98}5d^{4.84}6p^{0.04}7s^{0.01}6d^{0.03}\ 7p^{0.01}$	0.14
	C_5	$2s^{1.65}2p^{2.99}3p^{0.03}$	–0.66		W_3W_7	$6s^{1.07}5d^{5.10}6p^{0.06}6d^{0.02}$	–0.22
W_4C^-	W_1W_3	$6s^{1.39}5d^{4.79}6p^{0.07}7s^{0.01}6d^{0.02}$	–0.25		W_4	$6s^{1.07}5d^{5.11}6p^{0.06}6d^{0.02}$	–0.22
	W_2W_4	$6s^{1.00}5d^{4.79}6p^{0.06}7s^{0.01}6d^{0.02}7p^{0.01}$	0.15		W_5	$6s^{0.98}5d^{4.84}6p^{0.04}7s^{0.01}6d^{0.03}\ 7p^{0.01}$	0.14
	C_5	$2S^{1.65}2p^{3.12}3p^{0.03}$	–0.80		C_6	$2s^{1.53}2p^{3.20}3p^{0.03}$	–0.75
W_4C^+	W_1W_3	$6s^{0.77}5d^{4.77}6p^{0.03}7s^{0.01}6d^{0.01}$	0.45	W_6C^+	W_1	$6s^{0.68}5d^{4.85}6p^{0.03}6d^{0.02}$	0.46
	W_2	$6s^{0.71}5d^{4.69}6p^{0.05}6d^{0.01}$	0.56		W_2	$6s^{0.67}5d^{4.85}6p^{0.03}6d^{0.02}$	0.46
	W_4	$6s^{0.99}5d^{4.77}6p^{0.04}6d^{0.01}$	0.21		W_3W_7	$6s^{0.89}5d^{4.98}6p^{0.05}6d^{0.01}$	0.09
	C_5	$2s^{1.66}2p^{3.00}3p^{0.01}$	–0.68		W_4	$6s^{0.89}5d^{4.99}6p^{0.05}6d^{0.01}$	0.08
W_5C	W_1	$6s^{1.17}5d^{4.88}6p^{0.04}6d^{0.02}$	–0.08		W_5	$6s^{0.67}5d^{4.85}6p^{0.03}6d^{0.02}$	0.46
	W_2	$6s^{0.86}5d^{4.74}6p^{0.04}7s^{0.01}6d^{0.02}$	0.37		C_6	$2s^{1.54}2p^{3.08}3p^{0.03}$	–0.65

As shown in Table 3, The E^2 values in $WC^{0,\pm}$ dimer are small, but the WBI values are much larger. So the charge transfer can be attributed to the strong covalent bond. For the $W_2C^{0,\pm}$ cluster, the values of E^2 are much larger so that charge transfer mainly arises from donor–acceptor interaction. For $n > 2$ cluster series, as the number of donor–acceptor interaction and covalent bond increases it is difficult to distinguish the main interaction patterns, we can say that the charge transfer is ascribed to the above two interaction patterns.

Moreover, through comparing the different neutral, anionic and cationic charges within the same cluster size, we find that attached electron charges distributed to the C atom change from 30% when the cluster size $n = 1$ to 5% when the cluster size $n = 6$, and the remaining part of the additive electron charges are distributed to the W atoms. The proximate changing trend can also be found in the case of ionized electron. To further understand this phenomenon, we perform a detailed analysis of the highest occupied molecular orbital (HOMO) and the lowest unoccupied molecular orbital (LUMO) of $W_nC^{0,\pm}$ (n = 1–6) clusters. The C atom for the orbital percentage composition decreases from about 30% when the cluster size $n = 1$ to 4% when the cluster size $n = 6$, which is consistent with electron distribution. Therefore, the change trend of electron charges distributed on C atom may be due to the contributions of HOMO and LUMO orbitals.

Table 3. Primary E^2 and WBI of $W_nC^{0,\pm}$ (n = 1, 2) clusters.

Cluster	Donor	Acceptor	e_{occ}			E^2/(kcal/mol)			WBI_{W-C}
			α	β	Total	α	β	Total	
WC	CR (W)[a]	π^*_{W-C}	0.019	0.019	0.038	27.29	28.97	56.26	2.93
WC^-	CR(W)	π^*_{W-C}	0.013	0.013	0.026	14.00	13.73	27.73	3.06
WC^+	CR(W)	π^*_{W-C}	0.011	0.004	0.015	17.50	3.06	20.56	2.56
W_2C	LP*(W_1/ W_2)[b]	LP(C)[c]	0.369	0.369	0.738	160.79	160.79	321.58	1.50
W_2C^-	π_{W-C}	LP*(W)	0.293	0.288	0.581	63.52	62.66	126.18	1.54
W_2C^+	LP*(W_1/ W_2)	LP(C)	0.391	–	0.391	247.87	–	247.87	1.48
	π^*_{W-W}	LP*(C)	–	0.365	0.365	–	160.94	160.94	

[a]CR means core pair; [b]LP* means valence anti-bond lone pair; [c]LP means valence lone pair.

3.3. Spectrum analysis

In order to determine the structure of a cluster, regardless of whether by diffraction, electronic or vibrational spectroscopy, the comparison of the experimentally obtained spectra with simulated spectra is necessary. In this article, we use B3LYP/LANL2DZ method to calculate the infrared spectra for the ground state structures of $W_nC^{0,\pm}$ (n = 2–6) clusters, which is able to interpret the spectra in terms of the cluster structures once the experimental spectra have been recorded.

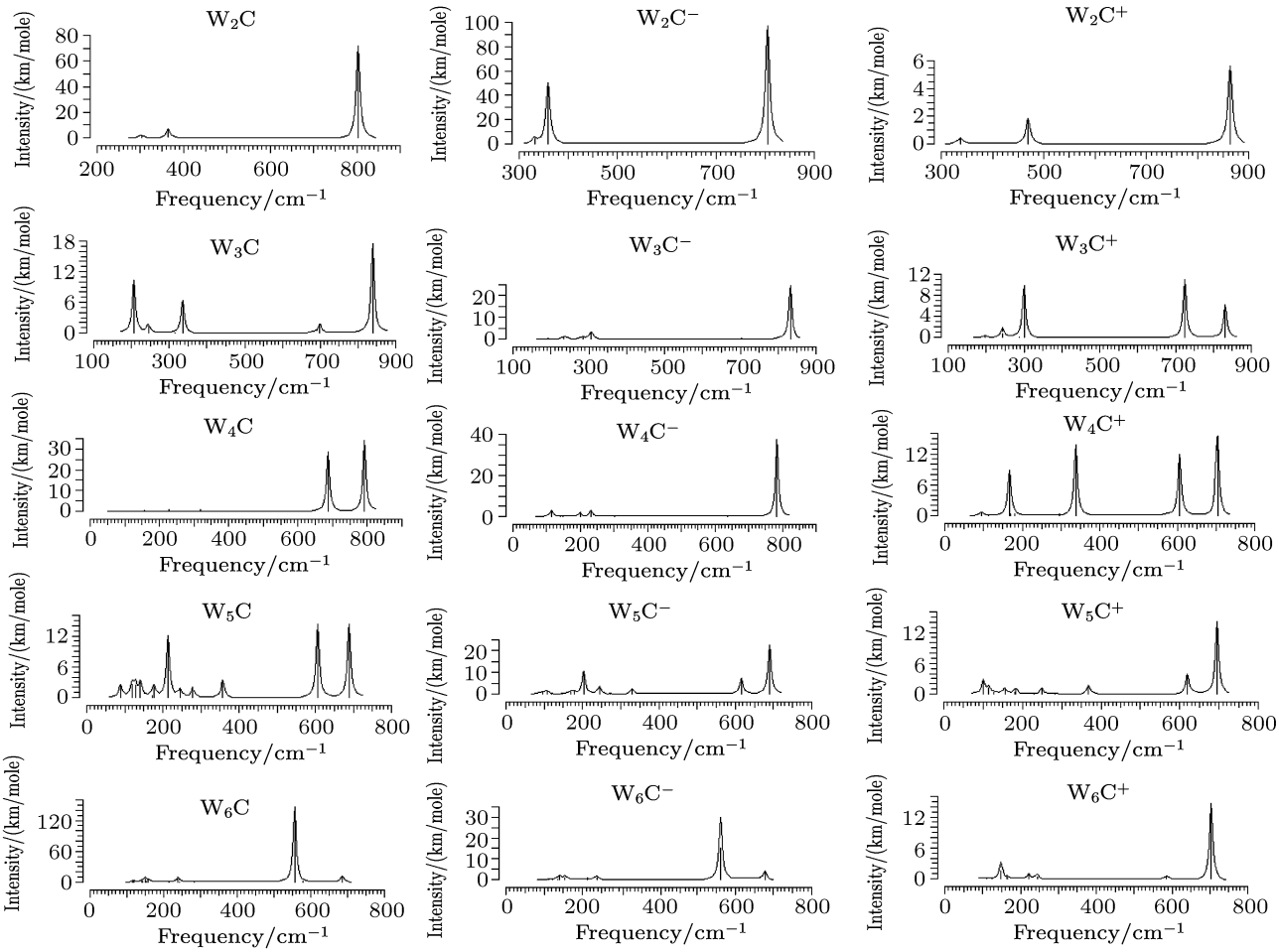


Fig. 2. Calculated IR spectra of $W_nC^{0,\pm}$ (n = 2–6) clusters.

The simulated IR spectra of $W_nC^{0,\pm}$ (n = 2–6) clusters are shown in Fig. 2. The IR spectra of the neutral and anion clusters show strong peaks at 802 cm^{-1} and 805 cm^{-1} for the $W_2C^{0,\pm}$ clusters and at 863 cm^{-1} for the cationic cluster, corresponding to a blue-shift of 61 cm^{-1} compared with the IR spectrum peak of the neutral cluster, because the W–C bond length of 1.94 Å (1 Å=0.1 nm) for the cationic cluster is shorter than that of 1.99 Å for the neutral cluster, a stronger W–C bond exists in the cationic cluster. The $W_2C^{0,\pm}$ cluster vibration modes of strong peaks may be assigned to the stretching of the C atom. Also, a weak peak at 359 cm^{-1} appears in W_2C^- due to the C atom in-plane wagging vibration, which can be used as a signal to identify the W_2C and W_2C^- clusters.

For the neutral W_3C cluster, there are three obvious peaks, the strongest peak at 838 cm^{-1} is assigned to the stretching of the C atom; the double-degenerate peak at 206 cm^{-1} is assigned to the W_3 atom in-plane wagging vibration; and the triply degenerate peak at 335 cm^{-1} is assigned to C atom out-of-plane wagging vibration. In the IR spectrum of W_3C^-, there is one peak at 832 cm^{-1}, whose vibration mode is the stretching of the C atom. In the IR spectrum of W_3C^+, the two strongest peaks at 300 cm^{-1} and 724 cm^{-1}, whose vibration modes are C atom out-of-plane wagging and in-plane wagging. The medium intensity of the C atom stretching mode is due to the decrease of electron on W–C bond.

For the neutral W_4C cluster, there are two strong peaks, the strongest peak at 791 cm^{-1} is assigned to the stretching of the C atom, the second peak at 687 cm^{-1} is due to the C atom in-plane wagging, the C atom stretching mode gives rise to the strongest peak in W_4C^- and W_4C^+, but their vibrational frequencies are different. The frequency of W_4C^- is similar to that of the neutral cluster, while W_4C^+ is red-shifted by as much as 87 cm^{-1}, which is related to the fact that its W–C bond length is larger than that for neutral and anionic clusters. In the W_4C^+ cluster, besides three C atom vibration modes from 338 cm^{-1} to 704 cm^{-1}, there is a new vibration mode at 167 cm^{-1} that is caused by the W_3 atom stretching vibration.

For the neutral W_5C cluster, there are the two strongest peaks at 606 cm^{-1} and 689 cm^{-1}, whose vibration modes are C atom out-of-plane wagging and stretching vibration. Another strong peak appears around 213 cm^{-1}, which comes from W_3 and W_4 atom stretching deformation. More interestingly, because of tungsten atom number increase and C_1 symmetry, the IR spectrum of the W_5C cluster shows several low-frequency peaks, which can also be seen in $W_5C^-$and W_5C^+ clusters. The strongest peaks of W_5C^- and W_5C^+ clusters are located at 690 cm^{-1} and 695 cm^{-1}, which are both assigned to the C atom stretching vibration. In addition, there is a weak peak at 203 cm^{-1} resulting from structural distortion in W_5C^-, which can be used to identify W_5C^- and W_5C^+ clusters.

For the neutral W_6C cluster, the peak at 556 cm^{-1} comes from the C atom wagging vibration. For W_6C^- cluster, the peak appears around 562 cm^{-1}, which is, in fact, composed of two vibration modes at 561.8 cm^{-1} and 561.9 cm^{-1}, coming from C atom vertical and lateral waggings. As for W_6C^+ cluster, the peak appears at 704 cm^{-1}, whose vibration mode is C atom stretching vibration.

From the IR spectra of $W_nC^{0,\pm}$ (n = 2–6) clusters, we can see that the vibrational frequencies are in a range of 80 cm^{-1}–864 cm^{-1}, similar to those of $W_nSi_2{}^{0,\pm}$ (n = 1–5) clusters.[34] The high frequency, strong peak modes are found to be almost entirely due to the stretching deformation of the carbide atom. This is caused mainly by two aspects: firstly, the strong interaction between W and C atoms; and, secondly, the C atom is the major carrier of negative electrons, so the change of electric dipole moment for $W_nC^{0,\pm}$ (n = 2–6) clusters is the biggest on the condition of C atom stretching vibration.

3.4. Polarizability

It is known that the static dipole polarizability is a measure of the distortion of the electronic density and the information about the response of the system under the action of an external static electric field. The dipole polarizability and the polarizability anisotropy are computed using the B3LYP/LANL2DZ method.

The dipole polarizability ($\langle\alpha\rangle$) and the polarizability anisotropy ($\Delta\alpha$) are defined as

$$\langle\alpha\rangle = \frac{1}{3}\left(\alpha_{xx} + \alpha_{yy} + \alpha_{zz}\right), \tag{1}$$

$$\Delta\alpha = \left[\frac{\left(\alpha_{xx} - \alpha_{yy}\right)^2 + \left(\alpha_{yy} - \alpha_{zz}\right)^2 + \left(\alpha_{zz} - \alpha_{xx}\right)^2 + 6\left(\alpha_{xy}^2 + \alpha_{xz}^2 + \alpha_{zy}^2\right)^2}{2}\right]^{1/2}. \tag{2}$$

The results of $\langle\alpha\rangle$ and $\Delta\alpha$ for $W_nC^{0,\pm}$ ($n = 1$–6) clusters are shown in Figs. 3 and 4, respectively. It is intriguing that $\langle\alpha\rangle$ increases linearly with the number of tungsten atoms increasing. A similar behaviour was observed in the gold cluster.[35] Within the same cluster size, the $\langle\alpha\rangle$ order is anionic>neutral>cationic. Karamanis *et al.*[36] have shown that a more polarizable cluster is characterized by smaller Al atom average natural charge ($\overline{q}_{Al}$) for Al_nP_n clusters. In our cluster system, from Table 3, we can easily find that W atom average natural charge in cationic clusters is the largest but it is the smallest in anionic clusters with the same size, so that the $\langle\alpha\rangle$ order phenomenon can be described.

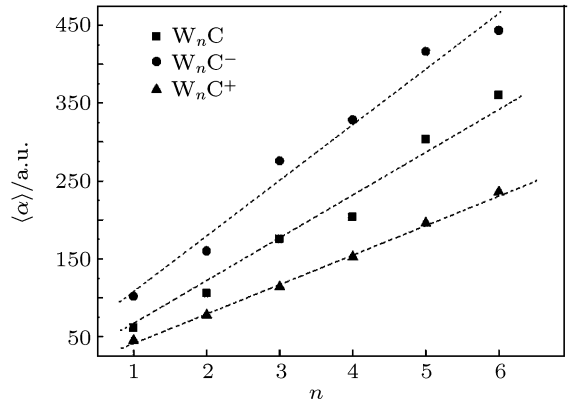


Fig. 3. Calculated values of dipole polarizability ($\langle\alpha\rangle$) for $W_nC^{0,\pm}$ ($n = 1$–6) clusters.

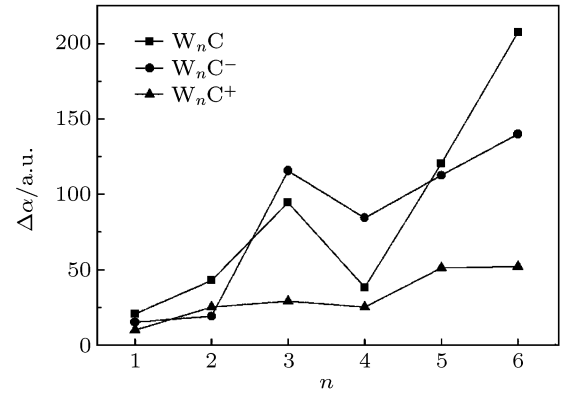


Fig. 4. Calculated values of polarizability anisotropy ($\Delta\alpha$) for $W_nC^{0,\pm}$ ($n = 1$–6) clusters.

The polarizability anisotropies of $W_nC^{0,\pm}$ ($n = 1$–6) clusters increase for $n = 1$–3 and decrease when $n = 4$. For $n > 4$ neutral and anionic clusters, there is a monotonic increase in polarizability anisotropy value. We can find that polarizability anisotropy is directly related to the particular cluster structure. For example, in the planar structure cluster it increases with the number of tungsten atoms increasing. When $n = 4$, the polarizability anisotropies decreases because the cluster structure becomes three-dimensional and it increases again except for W_6C^+ cluster (due to its highly C_{3v} symmetry and compact structure).

4. Conclusion

In this work, we gave a systematic theoretical study of $W_nC^{0,\pm}$ ($n = 1$–6) clusters using the DFT method. According to the carefully optimized geometries, we calculated the electronic structure, the infrared vibration spectrum and the static polarizability for $W_nC^{0,\pm}$ ($n = 1$–6) clusters. Our results are summarized as follows.

(i) The ground state structures of neutral, anionic and cationic clusters are similar within the same size, constituted by substituting the C atom for one W atom in the structures of W_{n+1} clusters. When $n > 3$, the clusters undergo a transition from two-dimensional structure to three-dimensional structure.

(ii) The detailed natural (NBO) charge analyses indicate that the direction of charge transfer is from W atom to 2p orbital of C atom, and strong donor–acceptor interaction and covalent bond are used to interpret the charge transfer.

(iii) From the infrared spectra of $W_nC^{0,\pm}$ ($n = 2$–6) clusters, we can see the vibrational frequencies of neutral, anionic and cationic clusters are similar in a range of 80 cm^{-1}–864 cm^{-1}. The high frequency, strong peak modes are found to be almost stretching deformation of the carbide atom.

(iv) Polarizability increases linearly with the number of tungsten atoms increasing.

References

[1] Pol S V, Pol V G and Gedanken A 2006 *Adv. Mater.* **18** 2023

[2] Keller N, Pietruszka B and Keller V 2006 *Mater. Lett.* **60** 1774

[3] Zhao Z G and Miyauchi M 2008 *Angew. Chem. Int. Ed.* **47** 7051

[4] Karre P S K, Acharya M, Knudsen W R and Bergstrom P L 2008 *IEEE Sens. J.* **8** 797

[5] Kida T, Nishiyama A, Yuasa M, Shimanoe K and Yamazoe N 2009 *Sensor. Actuat.* B: *Chem.* **135** 568

[6] Liang C, Ding L, Wang A, Ma Z and Qiu J 2009 *Ind. Eng. Chem. Res.* **48** 3244

[7] Guo Z, Lu B, Jiang X and Zhao J J 2011 *Acta Phys. Sin.* **60** 013601 (in Chinese)

[8] Gu J, Wang S Y and Gou B C 2009 *Acta Phys. Sin.* **58** 3338 (in Chinese)

[9] Scharf T W, Romanes M C, Mahdak K C, Hwang J Y, Banerjee R, Evans R D and Doll G L 2008 *Appl. Phys. Lett.* **93** 151909

[10] Abad M D, Sánchez-López J C, Cusnir N and Sanjines R 2009 *J. Appl. Phys.* **105** 033510

[11] Weidele H, Kreisle D, Recknagel E, Icking-Konert G S, Handschuh H, Gantefor G and Eberhardt W 1995 *Chem. Phys. Lett.* **237** 425

[12] Zhang X R, Ding X L, Dai B and Yang J L 2005 *J. Mol. Struct.: Theochem* **757** 113

[13] Zhang X R, Ding X L and Yang J L 2005 *Int. J. Mod. Phys.* B **19** 2427

[14] Du J, Sun X, Meng D, Zhang P and Jiang G 2009 *J. Chem. Phys.* **131** 044313

[15] Borin A C, Gobbo J P and Roos B O 2010 *Chem. Phys. Lett.* **490** 24

[16] Sherrill C D and Piecuch P 2005 *J. Chem. Phys.* **122** 124104

[17] Olga G and Leeor K 2007 *J. Chem. Phys.* A **111** 2028

[18] Wang X R and Zheng H P 2009 *Chin. Phys.* B **18** 1968

[19] Zhang C R, Chen H S, Song Y and Xu G J 2007 *Chin. Phys.* **16** 2394

[20] Shane M S, Adam W S and Michael D M 2002 *J. Chem. Phys.* **116** 993

[21] Fei Q, Liu S, Hui G and Yun Z 1999 *Acta Chim. Phys. Sin.* **12** 525

[22] Li X, Liu S S, Chen W and Wang L 1999 *J. Chem. Phys.* **111** 2464

[23] Rothgeb D, Hossain E and Jarrold C C 2008 *J. Chem. Phys.* **129** 114304

[24] Samuel J, Peppernick K D, Gunaratne D and Castleman A W 2010 *Chem. Phys. Lett.* **489** 1

[25] Balasubramanian K 2000 *J. Chem. Phys.* **112** 7425

[26] Stevens F, Carmichael I, Callens F and Waroquier M 2006 *J. Chem. Phys.* A **110** 4846

[27] Wang J, Sun X and Wu Z 2007 *J. Cluster Sci.* **18** 333

[28] Zhang X R, Ding X L, Fu Q and Yang J L 2008 *J. Mol. Struct.: Theochem* **867** 17

[29] Frisch M J, Trucks G W, Schlegel H B, Scuseria G E, Robb M A, Cheeseman J R, Montgomery Jr J A, Vreven T, Kudin K N, Burant J C, Millam J M, Iyengar S S, Tomasi J, Barone V, Mennucci B, Cossi M, Scalmani G, Rega N, Petersson G A, Nakatsuji H, Hada M, Ehara M, Toyota K, Fukuda R, Hasegawa J, Ishida M, Nakajima T, Honda Y, Kitao O, Nakai H, Klene M, Li X, Knox J E, Hratchian H P, Cross J B, Adamo C, Jaramillo J, Gomperts R, Stratmann R E, Yazyev O, Austin A J, Cammi R, Pomelli C, Ochterski J W, Ayala P Y, Morokuma K, Voth G A, Salvador P, Dannenberg J J, Zakrzewski V G, Dapprich S, Daniels A D, Strain M C, Farkas O, Malick D K, Rabuck A D, Raghavachari K, Foresman J B, Ortiz J V, Cui Q, Baboul A G, Clifford S, Cioslowski J, Stefanov B B, Liu G, Liashenko A, Piskorz P, Komaromi I, Martin R L, Fox D J, Keith T, Al-Laham M A, Peng C Y, Nanayakkara A, Challacombe M, Gill P M W, Johnson B, Chen W, Wong M W, Gonzalez C and Pople J A 2003 *Gaussian* 03 Revision B.04, Gaussian, Inc., Pittsburgh, PA

[30] Hay P J and Wadt W R 1985 *J. Chem. Phys.* **82** 270

[31] Zhang Z X, Cao B B and Duan H M 2008 *J. Mol. Struct.: Theochem* **863** 22

[32] Gutsev G L and Bauschlicher C W 2003 *Chem. Phys.* **291** 27

[33] Zhang X R, Liu X F and Kang Z L 2010 *J. At. Mol. Phys.* **27** 869 (in Chinese)

[34] Zhang X R, Gao C H, Wu L Q and Tang H S 2010 *Acta Phys. Sin.* **59** 5429 (in Chinese)

[35] Li X, Wang H, Yang X, Zhu Z and Tang Y 2007 *J. Chem. Phys.* **126** 084504

[36] Karamanis P, Xenides D and Leszczynski J 2008 *J. Chem. Phys.* **129** 094708